Thermal Aging of Undoped Polyaniline: Effect of Chemical Degradation on Electrical Properties

Yannick Kieffel,[1] Jean Pierre Travers,[1] Anne Ermolieff,[2] Denis Rouchon[2]

[1]*Laboratoire de Physique des Métaux Synthetiques UMR 5819 (CEA-CNRS-UJF), Département de Recherche Fondamentale sur la Matière Condensée, CEA Grenoble, 38054 Grenoble, Cedex 9, France*
[2]*CEA-LETI DTS/SCPC, 38054 Grenoble, Cedex 9, France*

Received 1 June 2001; accepted 2 January 2002

ABSTRACT: Aging experiments, with a special emphasis on the atmosphere effect, have been carried out on undoped polyaniline, in its half-oxidized state, namely emeraldine base (EB). The polymer has been aged under vacuum and in air atmosphere. The chemical degradation has been analyzed by several complementary techniques such as viscosity measurements, FTIR, XPS, and UV-Vis-nIR spectroscopy. We show that emeraldine base exhibits two different degradation mechanisms. The first one is intrinsic to the polymer and occurs independently on aging conditions (vacuum or air). It consists of crosslinking via tertiary amine groups created from imine nitrogen via double-bond breaking. The second mechanism is extrinsic and occurs concomitantly with the first one upon aging in air. It consists of oxygen incorporation in a form of carbonyl groups and chain scission. Both degradation pathways result in a decrease of the electrical conductivity of the polymer due to the lowering of the average conjugation length. © 2002 Wiley Periodicals, Inc. J Appl Polym Sci 86: 395–404, 2002

Key words: conjugated polymers; ageing; crosslinking; degradation

INTRODUCTION

Although polyaniline (PANI) has been known for more than hundred years, it has received renewed interest as an environmentally stable conducting polymer with potentials for use in a variety of applications. As in the case of other conducting polymers, the electrical conductivity of polyaniline can be controlled over many orders of magnitude through acid-base or redox type doping.[1] The latter can be carried out either chemically or electrochemically.

Due to its excellent environmental stability in the undoped as well as in the doped state, polyaniline in its oxidation state of emeraldine base (EB) is considered as a very promising candidate for several industrial applications. For these reasons several industrial companies are presently involved in the production and testing of PANI. In the past, the principal industrial applications involved the doped form of the polymer with the goal to achieve the highest possible conductivity.[2] Nowadays, research interests are also directed towards undoped PANI which exhibits semiconducting properties.[3] The most important applications envisioned are: materials for charge transport layers in electroluminescent device,[4] stress grading material for high voltage cables,[5] and others.

For doped polyaniline several articles dealing with aging studies were published.[6–10] These studies demonstrate that the degradation involves principally the removal of the dopant, accompanied by irreversible structural changes in the polymer chain, which in turn, lead to an irreversible drop in conductivity. Surprisingly, few aging studies have been carried out on undoped polyaniline (EB).[11–13]

We have undertaken such studies with the goal to determine the role of atmosphere constituents and especially oxygen in the degradation process. A combination of several chemical and spectroscopic techniques was used to follow the degradation process, namely elemental analysis, viscosimetry, IR spectroscopy, and XPS. The results are discussed in terms of the conjugation length decrease and its effect on the conductivity.

EXPERIMENTAL

Material

EB purchased from AC&T (St Egrève, France) was synthesized by chemical polymerization in aqueous HCl medium at −5°C using $(NH_4)_2S_2O_8$ as the oxidizing agent. The resulting polyaniline hydrochloride, PANI–HCl [commonly termed Emeraldine-Salt (ES)] was washed with water and dried at 40°C until constant mass. The polymer prepared in a such manner shows the conductivity of few $S \cdot cm^{-1}$. ES was then dedoped in NaOH aqueous solution (1 $mol \cdot L^{-1}$) to

Correspondence to: Y. Kieffel.
Contract grant sponsor: MENRT (French government).

Journal of Applied Polymer Science, Vol. 86, 395–404 (2002)

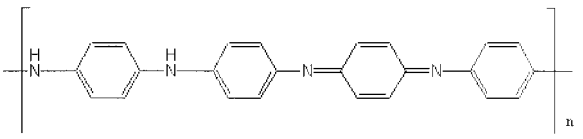

Figure 1 Emeraldine base structure.

obtain emeraldine base. The synthesized polymer, EB, is schematically depicted in Figure 1.

Viscosimetric studies

The inherent viscosity of EB at different stages of degradation was determined using an automatic Ubbelhode viscosimeter. The measurements were carried out at 25°C in 0.1 wt/wt % solution of the polymer in 97% sulfuric acid. EB solutions were stirred for c.a. 15 h prior to the measurement.

Fourier transform infrared spectroscopy

Fourier Transform Infrared spectra (FTIR) of EB powder were recorded, in the range of 400–4000 cm^{-1}, on a Perkin-Elmer Paragon 500 spectrometer using a diffuse reflectance technique. The application of this technique enables us to analyze the polymer directly in the form of powder without the necessity to mix it with KBr.

X-ray photoelectron spectroscopy

Aging-induced chemical changes in EB were also analyzed by X-ray Photoelectron Spectroscopy (XPS) on an ESCA SSI spectrometer using A1 Kα monochromatic radiation. The spot size was 250 $\times$ 1000 μm^2, the X-ray source power 300 W (10 kV $\times$ 30 mA), the take-off angle 35°, and the estimated sampling depth $\approx$10 nm. The pressure in the analyze chamber was maintained at 10^{-9} Torr. All binding energies were normalized with respect to Cls neutral carbon peak at 285 $\pm$ 0.1 eV to compensate for charge surface effects that occur in poorly conducting systems. The spectra were deconvoluted assuming 100% Gaussian peaks and a Shirley background.

Ultraviolet-visible spectroscopy (UV-Vis-nIR)

Uv-Vis-nIR absorption spectra were recorded on a Perkin-Elmer Lambda 900 spectrometer in the range of 250–1000 nm. EB powder was solubilized in NMP, and the nonsoluble fraction was separated by centrifugation.

Conductivity measurements

Conductivity was measured on 200 μm-thick pressed pellets that were sandwiched between two evaporated gold electrodes of 6-mm diameter. Current density vs. electric field characteristics were measured at room temperature by a Keithley Model 6517A electrometer. Ohmic behavior was verified in each case.

RESULTS

In Table I the results of elemental analysis of pristine EB are presented. The main contamination are sulfur (0.13 wt %) and chlorine (0.20 wt %). One also observes a significant amount of oxygen (4.12 wt %). This problem will be addressed later. Both contaminating elements originate from the reaction mixture used for the synthesis. The source of chlorine is HCl, used to keep the reaction medium acidic, which, in addition, protonates the polymer formed upon oxidative polymerization. Thus, a small amount of Cl may be due to incomplete deprotonation, but other mechanisms involving covalently bonded chlorine cannot be totally excluded. Sulfur originates from the oxidizing-polymerizing agent [$(NH_4)_2S_2O_8$)], which is transformed into $(NH_4)_2SO_4$ in the course of the polymerization reaction. The presence of S in the elemental analysis must therefore involve the presence of oxygen in the molar ratio S:O = 1:4. This corresponds to 0.26 wt % of oxygen. Thus, the overall purity of the polymer can be calculated as 99.41 wt %. After the substraction of the contamination the chemical composition of EB is C: 76.39 wt %, N: 14.77 wt %, H: 4.95 wt %, and O: 3.88 wt %, which is in strong discrepancy with theoretical composition of EB ($C_6H_{4.5}N_1$), i.e., C: 77.84 wt %, H: 4.86 wt %, and N: 17.30 wt %. The formula that cor-

TABLE I
Elemental Analysis of EB Aged in Air at 140°C

	Elemental analysis						Chemical composition*					
Aging time (h)	C (wt %)	N (wt %)	H (wt %)	S (wt %)	Cl (wt %)	O (wt %)	C	N	H	S	Cl	O
0	75.94	14.69	4.92	0.13	0.20	4.12	6.03	1.00	4.69	0.0039	0.0054	0.24
24	77.04	14.94	4.68	0.06	0.17	3.11	6.01	1.00	4.38	0.0018	0.0045	0.18
96	76.88	14.94	4.60	0.06	0.22	3.30	6.00	1.00	4.31	0.0018	0.0058	0.19
960	74.32	14.78	4.25	0.06	0.25	6.34	5.86	1.00	4.02	0.0018	0.0067	0.37
1920	69.85	14.62	3.99	0.07	0.25	11.22	5.57	1.00	3.82	0.0021	0.0068	0.67

[a]Chemical composition of EB with 100% purity: C = 6.00, N = 1.00, H = 4.50, S = 0, Cl = 0, O = 0.

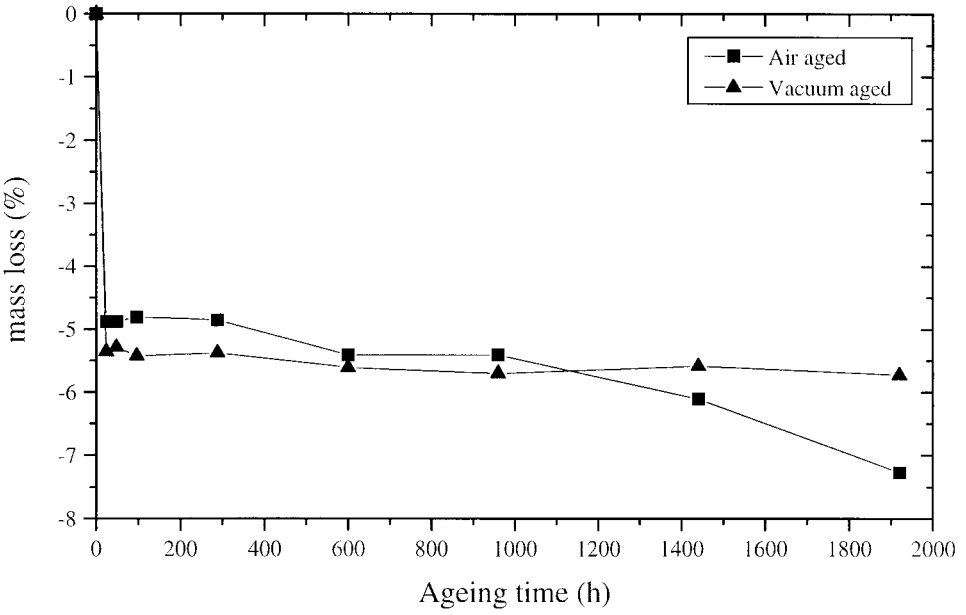

Figure 2 Mass loss of polyaniline powder aged in air (■), and under vacuum (▲) at 140°C.

responds to the elemental analysis is $C_6H_{4.69}N_1O_{0.23}$. The presence of oxygen and a significant excess of hydrogen are indicative of the presence of water in EB. It is known that EB is a hygroscopic material, and may absorb up to 5 wt % of water. The best fit between the calculated and analytically determined formula is found for the composition of $C_6H_{4.5}N_1(H_2O)_{0.23}$ corresponding to 4.3 wt % of water adsorbed in EB. It has been shown by DTA (Differential Thermal Analysis) and DSC (Differential Scanning Calorimetry) measurement that the residual water can be reversibly adsorbed in EB in two forms:[14] some H_2O molecules are weakly bonded to the amine nitrogen center acting as acceptors of protons (activation energy of 3–5 kcal/mol). Others are strongly bonded to the imine nitrogens acting as donors of protons (activation energy of 15–18 kcal/mol). In our case, we suppose that the residual water present in EB is strongly bonded to imine nitrogen, because the sample was pumped for extended time prior to elemental analysis.

Emeraldine base, has been aged, in a powder form, at the temperature of 140°C either in air or under dynamic vacuum (10^{-6} mbar). In Figure 2, the mass of the powder is plotted vs. the aging time, for both air and vacuum aged samples. For short aging times, an abrupt loss of mass is observed for both aging atmospheres. Elemental analyses show, in Table I and in Table II, a decrease in the oxygen and hydrogen contents, what can unequivocally be ascribed to the departure of the residual water. We can notice that the departure of water determined by elemental analysis does not match the mass loss measured by the thermogravimetric analysis. We suppose that during the manipulations preceding the elemental analysis water is readsorbed. For longer aging time, in the case of vacuum-aged samples, the mass remains then essentially unchanged even for times approaching 2000 h, which is in perfect agreement with elemental analysis results, which show very little composition changes for vacuum aged samples. In the case of air-aged samples, a different picture emerges. First, the mass decreases continuously with the increasing time, and second, a small acceleration of the mass loss is observed for aging times exceeding 1000 h. In elemental analysis data, a steady decrease in carbon content accompanied by a steady increase in oxygen content

TABLE II
Elemental Analysis of EB Aged under Vacuum at 140°C

	Elemental analysis						Chemical composition					
Aging time (h)	C (wt %)	N (wt %)	H (wt %)	S (wt %)	Cl (wt %)	O (wt %)	C	N	H	S	Cl	O
0	75.94	14.69	4.92	0.13	0.20	4.12	6.03	1.00	4.69	0.0039	0.0054	0.24
24	77.11	14.95	4.86	0.07	0.36	2.65	6.02	1.00	4.55	0.002	0.0095	0.16
96	77.29	15.00	4.86	0.04	0.40	2.41	6.01	1.00	4.54	0.0012	0.011	0.14
960	77.30	14.93	4.85	0.07	0.45	2.40	6.04	1.00	4.55	0.0021	0.012	0.14
1920	76.63	14.81	4.91	0.06	0.43	3.16	6.03	1.00	4.64	0.0018	0.011	0.19

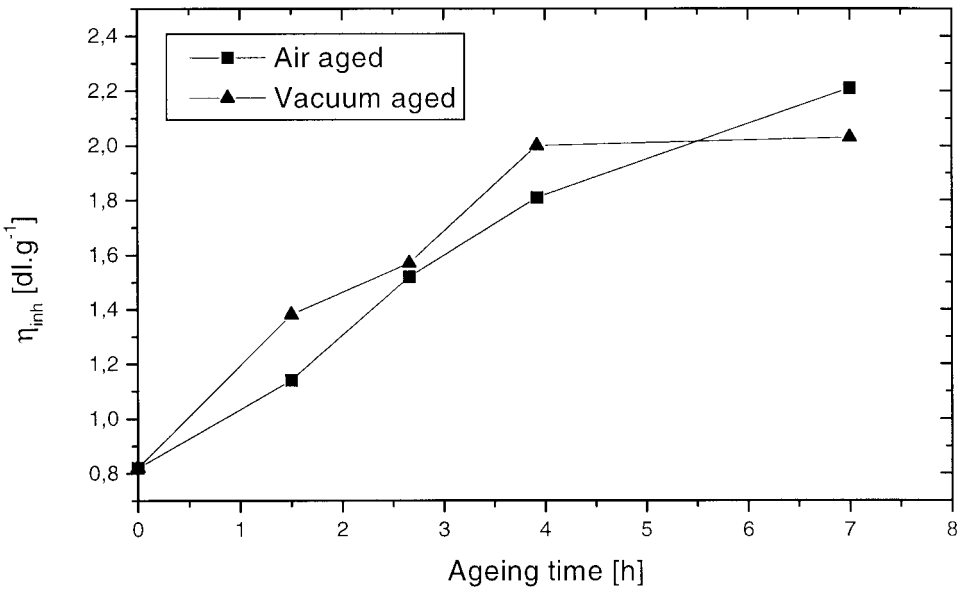

Figure 3 Intrinsic viscosity of EB aged at 140°C, in air (■), under vacuum (▲).

can be observed. The decrease in carbon content is indicative of chain scission phenomena involving the departure of small fragment containing CH groupings, whereas the increase of oxygen content can be interpreted in terms of chain oxidation.[15] Both processes have opposite effects on mass change in EB. Because the overall mass change is negative, the processes of chain scission must predominate. It should, however, be stressed that the above described processes account only for c.a. 2% of the total mass of the sample.

The evolution of the inherent viscosity, η_{inh}, of EB has also been investigated as a function of aging time for both air and vacuum aged samples. Actually, η_{inh} is connected to the viscosimetric molecular weight M_v by the Mark-Houwink relation (1),

$$\eta_{inh} = K[M_v]^a \quad (1)$$

with (K, a), the Mark-Houwink couple, which is constant for a given polymer/solvent/temperature system.[16,17] The value of a provides information about the conformation of the macromolecular chains. In the case of EB, it has been underlined that the relation between η_{inh} and M_v is linear, and a is close to 1.[18] This indicates that polyaniline adopts a rod-like conformation. Pristine EB exhibits $\eta_{inh} = 0.8\ dl \cdot g^{-1}$. The change of η_{inh} of polyaniline with aging time reflects its molecular weight changes. To characterize these changes, we have chosen intermediate aging times, namely 1, 2, and 4.5 h. An increase of η_{inh} with aging time can be observed (Fig. 3), which is indicative of an increase of the molecular weight of EB and irreversible structural changes. Because of the insolubility, in sulfuric acid, of samples aged for more than 24 h, the measurement of the inherent viscosity could not be performed for samples aged for extended time. The observed phenomena can be interpreted in terms of heavy crosslinking accompanying the aging, which leads to an increase in the molecular weight for samples aged for intermediate times. Further aging results in high crosslinking density, which in turn, makes the polymer insoluble in sulfuric acid. Evidently, chain scission occurrence, which can be deduced from elemental analysis and thermogravimetric measurements, is accompanied by the creation of crosslinked and/or branched structures probably via free radical-type coupling mechanism. It should be noted here that the above-described phenomena occur in air as well as in vacuum aged samples.

Elemental analysis and thermogravimetriy provide significant informations concerning the overall results of aging phenomena. However, specific changes accompanying the aging process should give rise to important changes in spectroscopic properties of the polymer. For these reasons we have undertaken a detailed IR and XPS studies of aged EB. For clarity of the discussion we discuss both cases of aging (air and vacuum) separately.

Aging under vacuum

IR spectra of pristine EB and polymer aged for different aging times are presented in Figure 4. In Table III, plausible peak assignments are listed. The spectrum measured in Figure 4 (a) is typical of polyaniline in the EB oxidation state. The band at ca. 1600 cm^{-1} can be attributed to C=C stretching in the quinoid type ring, whereas the band at 1510 cm^{-1} is due to a mixed

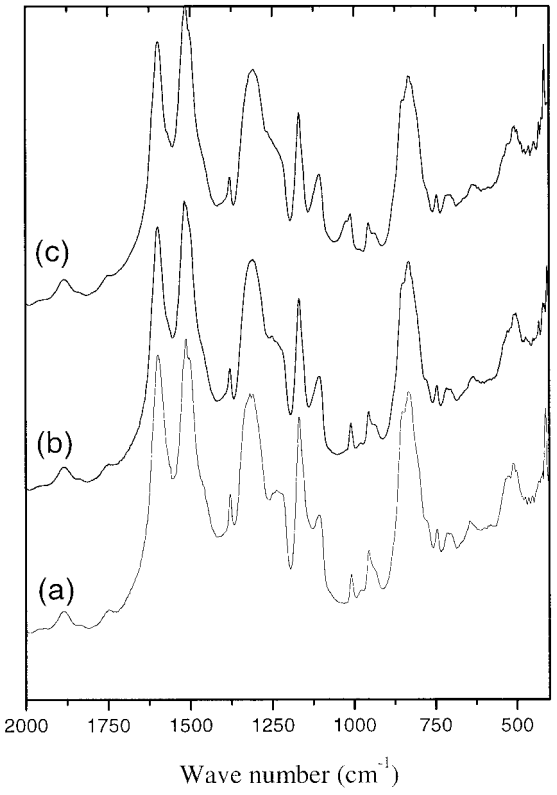

Figure 4 FTIR spectra of pristine EB (a), EB aged for 40 days under vacuum at 140°C (b), and EB aged for 80 days under vacuum at 140°C (c).

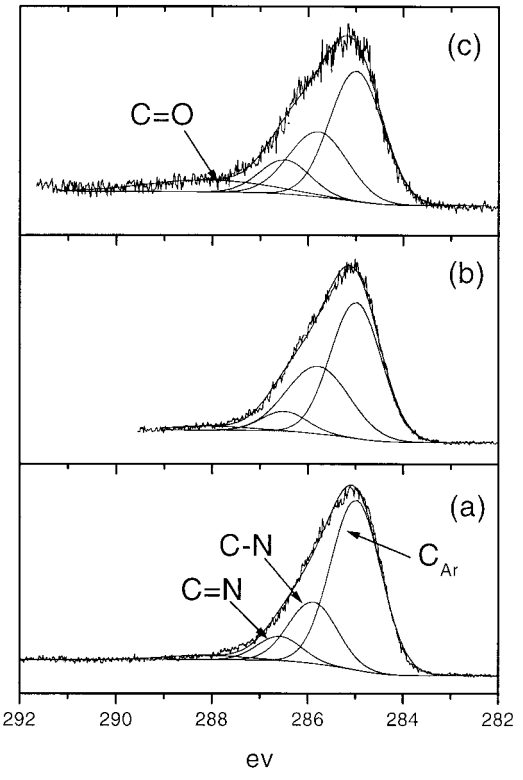

Figure 5 XPS Cls core level spectra of (a) pristine EB, (b) EB aged for 1920 h under vacuum at 140°C, and (c) EB aged for 1920 h in air at 140°C.

(C—C stretching + CH bending) mode of the benzenoid ring.[19] Aging causes a relative decrease in the intensity of the "quinoid" band (1600 cm^{-1}) with respect to the "benzenoid" one[20] (1510 cm^{-1}) [compare Fig. 4 (a) b and (c)]. This phenomenon can be correlated with a concomitant decrease of two bands at 1378 and 1310 cm^{-1}, which are also attributed to quinoid segments. In the same time a new peak appears at 1270 cm^{-1}, which can be assigned to the presence of tertiary amine.[21] The changes in IR spectra corroborate the crosslinking process, which must involve the formation of tertiary amines on the expense of imine nitrogens with simultaneous aromatization of quinoid rings.

TABLE III
FTIR Assignment

Wave number (cm^{-1})	Peak assignment
1600	Stretching of N=Q=N
1510	Stretching of N—B—N
1378	stretching of C—N in QB_tQ
1310	C—N stretching of QB_cQ, QBB, and BBQ
830	C—H out of the plan bending on 1.4-ring

Q: quinoïd unit, B: Benzenoïd unit, B_t: *trans* benzenoïd unit, B_c: *cis* benzenoïd unit.

The surface composition of EB has been investigated by XPS. First, we have characterized the surface composition of pristine EB, and then we have followed the surface composition changes induced by aging. Figure 5(a) shows the Cls spectrum of pristine EB. To a first approximation the spectrum can be fitted with four lines corresponding to four types of nonequivalent carbon atoms: the aromatic or quinone carbons bonded to hydrogen (C—H) at the bonding energy of 285 ± 0.1 eV, aromatic carbons bonded to amine nitrogen (C—N) at 285.8 ± 0.1 eV, quinone carbons bonded to imine nitrogen (C=N) at 286.5 ± 0.1 eV, and carbons of carbonyl groups (C=O) at 288.1 ± 0.1 eV.[22] The following composition of the surface can be established on the basis of Cls spectrum of pristine EB: C—H: 66%, C—N: 23%, C=N: 8% and C=O: 3%, which is slightly different than the theoretically predicted one, i.e., C—H: 66.66%, C—N: 25%, C=N: 8.33%. These results confirm that carbonyl groups are present even in nonaged polymer, at least on its surface. One must note, however, that the discrimination between a quinone type carbon atom bonded to nitrogen and an aromatic carbon atom bonded to nitrogen may be, in some cases, difficult due to small difference in the values of the energy of binding (EB) and large half-width of the peak.[22] For these reasons we carried out Nls XPS measurement, which give much clearer results. The Nls spectra were fitted using three contri-

butions: imine nitrogen (—N=C) at 398.8 ± 0.1 eV, secondary amine nitrogen at 399.9 ± 0.1 eV, and tertiary amine nitrogen at 400.8 ± 0.1 eV.[22–26] Alternatively the presence of this peak of low intensity can be attributed to incomplete dedoping of polyaniline, which shows the presence of Cl even in samples treated with NH_{3aq} for extended time and then carefully washed. In such a case this peak must originate from charged nitrogen species (—NH^+—) as postulated in refs, 10, 12, and 22. The Nls spectrum of pristine EB (Fig. 6) shows a somewhat higher number of secondary amine nitrogens (52%) than imine nitrogens (45%) with the presence of a small amount of tertiary amine nitrogen (3%), whereas theoretical values expected for EB oxidation state are 50% of secondary amine nitrogens, 50% imine nitrogens with nontertiary amine nitrogens. Aging-induced changes in XPS spectra are clearly visible [compare Fig. 5(a) and (b) and Fig. 6(a) and (b)]. After 1920 h of aging a significant increase of the content of tertiary amine nitrogens is observed, from 3 to 9%, with a simultaneous decrease of the imine nitrogen content (from 45 to 31%). Similar changes occur in the Cls spectra. The content of carbons connected to amine nitrogens (both secondary and tertiary) increases (from 25 to 34%) on the expense of imine nitrogens, whose content decreases from 8 to 7%.

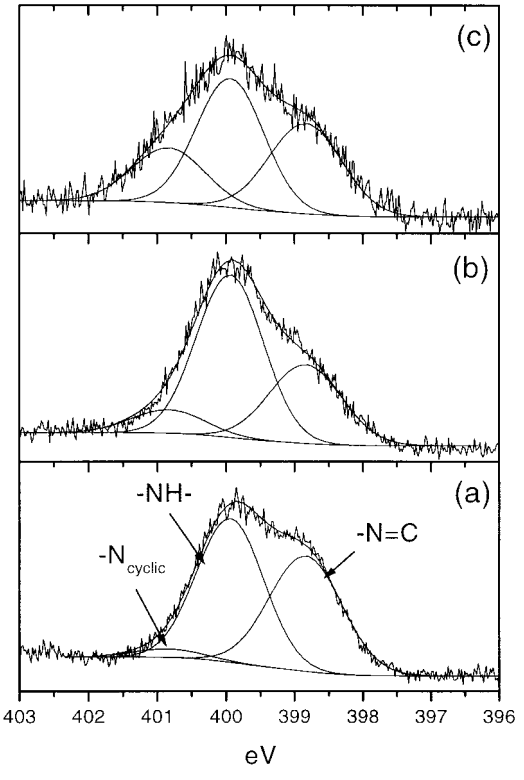

Figure 6 XPS Nls core level spectra of (a) pristine EB, (b) EB aged for 1920 h under vacuum at 140°C, and (c) EB aged for 1920 h in air at 140°C.

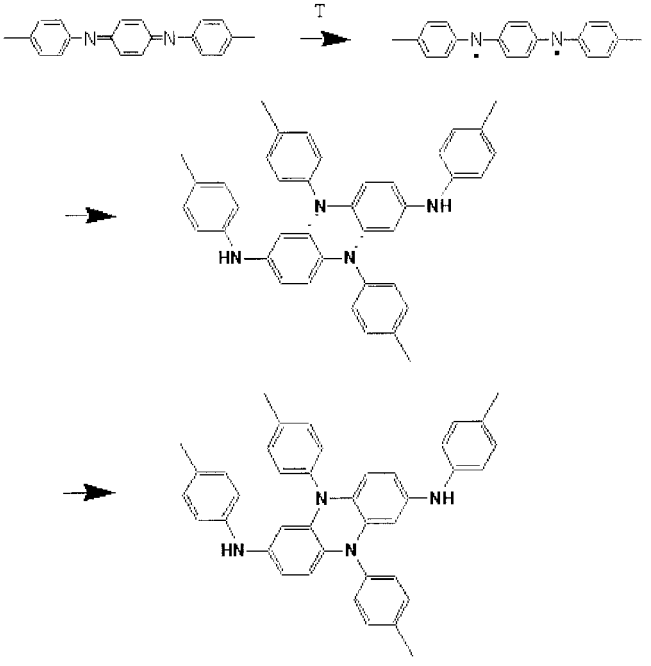

Scheme 1 Crosslinking mechanism in EB.

It should be underlined that the results of XPS are in very good agreement with those derived from IR studies, where similar trends were observed. We are tempted to propose the following explanation of the observed, aging-induced, spectroscopic changes. We suppose that at high temperature the C=N double bond breaks, leading to the aromatization of the quinoid ring with simultaneous formation of the free radicals. These free radicals may react with free radicals of an adjacent chain leading to the crosslinked polymer (Scheme 1), which becomes insoluble. The above-described mechanism of aging in oxygen-free atmosphere was first suggested by Scherr et al.[27]

Aging in air

IR spectra of EB aged in air are presented in Figure 7. Two distinctly different aging processes can be distinguished on the basis of the observed spectral changes. The first process is essentially the same as that observed for samples aged without the presence of oxygen, and can be described by the mechanism proposed by Scherr (vide supra). In particular, it is manifested by the decrease of the intensity of the IR bands associated with the quinoid rings (1600, 1378, and 1310 cm^{-1}) with respect to the peak attributed to the aromatic structure (1510 cm^{-1}). Similarly, the band due to tertiary amines appears at 1270 cm^{-1}. The influence of the presence of oxygen is manifested in this case, only as an acceleration of the crosslinking process.

The second aging process consists of the oxidation of the polymer chain with concomitant creation of carbonyl groups. The formation of carbonyl linkages

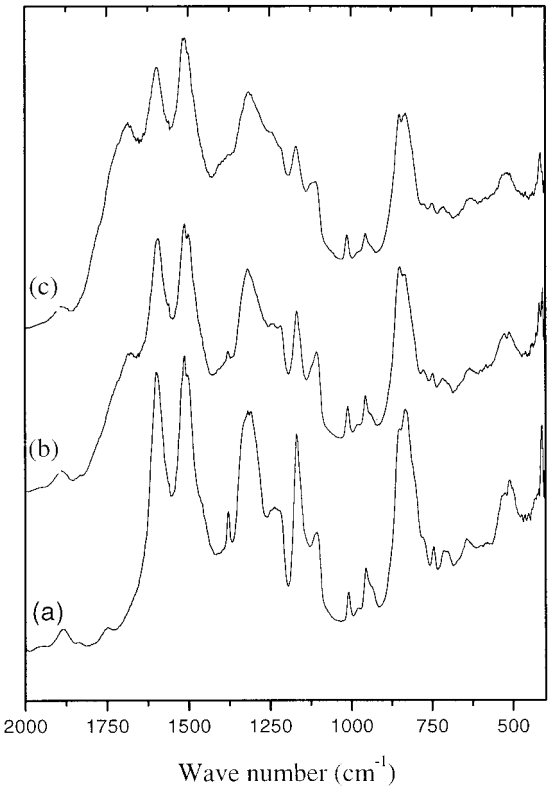

Figure 7 FTIR spectra of pristine EB (a), EB aged for 40 days in air at 140°C (b) and EB aged for 80 days in air at 140°C (c).

gives rise to an IR peak at 1680 cm^{-1}, whose intensity increases with the increase of the aging time.[21] A bathochromic shift in C=O stretching frequency to 1680 cm^{-1} is indicative of the fact that the double bond of the carbonyl group is in conjugation with the π bonding system of the polymer.

Cls XPS spectrum of the sample aged in air for 1920 h is shown in Figure 6 (c). The chemical composition of the polymer surface derived from this spectrum is as follows: C—H: 50%, C—N: 27%, C=N: 12% and C=O: 11%. Thus, a strong increase in the content of carbonyl functional groups is observed, which is consistent with IR investigations. One should, however, notice that the halfwidth of the line attributed to C=O is 3 eV, which implies that this peak could, in principle, be further decomposed. It is, therefore, possible that at the surface of the aged polymer, oxygen may be present in a form of other than carbonyl functional groups.[23,24] In the Nls core level spectrum, shown in Figure 6 (c), we observe a decrease of the imine and amine nitrogen concentrations (34 and 45%, respectively) and a strong increase of the tertiary amine nitrogen content (21%). The results clearly confirm the data obtained from IR spectroscopy and show that the crosslinking process proposed for EB aging in vacuum (Scheme 1) occurs also in samples aged in air. Again, it should be noted that the presence of oxygen accelerates the formation of tertiary amine type functional groups.

As it was stated above, the analysis of Cls spectra of nonaged and aged EB seems to indicate that several types of chemically nonequivalent oxygen containing groups may be present at the surface of the polymer. This hypothesis was confirmed by Ols spectra (Fig. 8). The most plausible decomposition of the spectra is as follows: ketone (C=O) at 531.9 ± 0.1 eV, hydroxyl, ether, and bonded water (C—O—H, C—O—C, H_2O) at 532.8 ± 0.1 eV and ester (O=C—O*—C) at 534 ± 0.1 eV (the asterisk corresponds to the analyzed oxygen).[28,29] Based on this assumption we can determine that the surface of pristine (nonaged) EB contains the following types of oxygen bearing groups: ketone 26%, hydroxyl, ether, and bonded water 38% and ester 36%. We observed by elemental analysis that oxygen in EB was mainly present in the form of residual water. By XPS we point out that the presence of oxygen has several origins: it is not only adsorbed at the surface in a form of water but also is present in oxidized segments, which are more abundant at the surface of the polymer. Both results are not necessarily inconsistent, because XPS is a surface analysis method that artificially enhances the content of oxidized segments that are more frequent at the surface of the polymer. We assume that the origin of this molecular

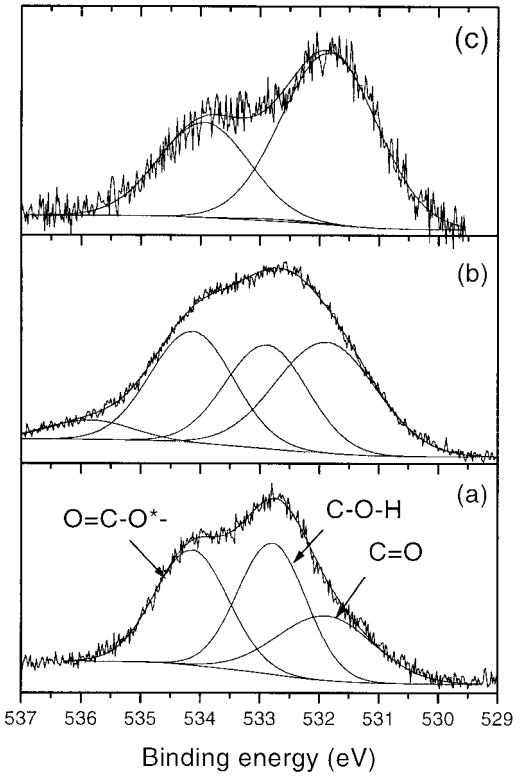

Figure 8 XPS Ols core level spectra of (a) pristine EB, (b) EB aged for 600 h in air at 140°C and (c) EB aged for 1920 h in air at 140°C.

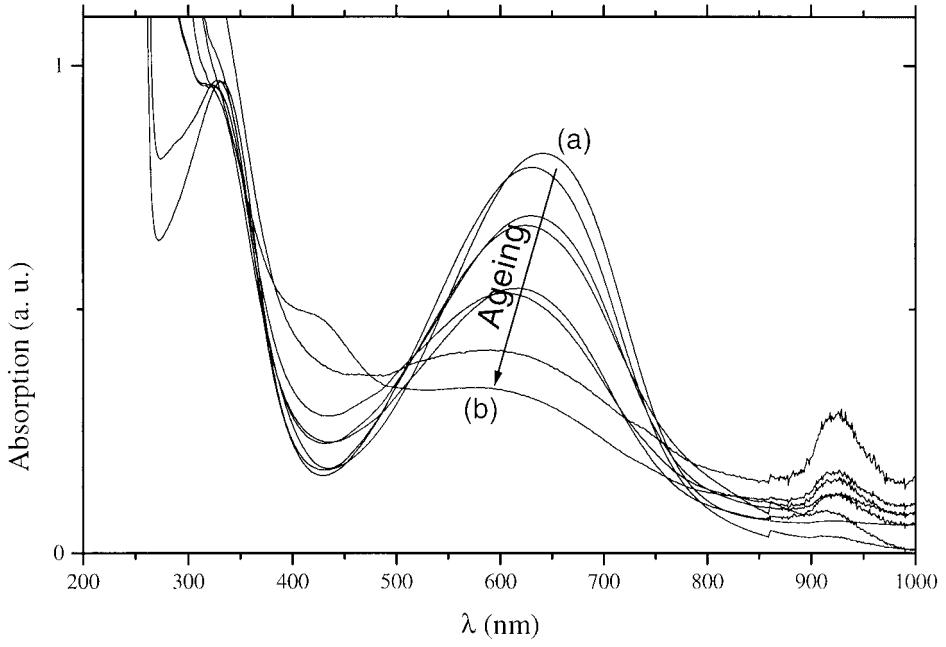

Figure 9 UV-Vis absorption spectra for (a) pristine EB and for EB aged in air at 140°C up to (b) 1440 h.

oxygen is due to the surface oxidation of EB powder during the stocking time. Because this oxidation affects only the surface, it is hardly detectable by elemental analysis. The evolution of the spectrum caused by aging can be characterized as follows: the content of ketone groups increases from 36% for the sample aged for 600 h to 65% for the one aged for 1920 h, the content of hydroxyl, ether, and bonded water decreases from 28% for the sample aged for 600 h to 0% for the one aged for 1920 h and the content of the esters remain constant with 30% for the sample aged for 600 h and 34% for the one aged for 1920 h. We assume that hydroxyls and ether are unstable in the oxidizing environment, and can be the precursor of oxidation leading to ketone or esters. The major part of oxygen is incorporated in the polymer chain in the form of ketone, which is consistent with IR results.

On the basis of IR and XPS spectroscopic experiments it is clear that aging in air induces a decreasing content of imine and secondary amine functional groups and an increasing content of tertiary amine ones. Thus, the degradation mechanism must be in this case of similar chemical nature as that elucidated for vacuum-aged EB. It consists of thermally induced breaking of π-bonds in imine groups with simultaneous creation of tertiary amine and, by consequence, crosslinking centers. This process is accelerated in the presence of oxygen. In addition to the catalytic role of oxygen in the formation of crosslinked structure one must postulate the phenomenon of oxygen incorporation to the polymer chain, predominantly in a form of ketone groups but also as surface-confined ester groups (vide supra). The results of elemental analysis (Table I) show that the content of incorporated oxygen may reach up to 7 wt % for 2000 h aging time in air at 140°C. It can also be correlated with the decrease in both carbon and hydrogen content. We suppose that the oxidation mechanism, which leads to the incorporation of oxygen, may also induce chain scission and the departure of small hydrocarbon fragments. This process can explain the loss of mass observed, in the thermogravetric study, for long aging time. We can notice that the mass loss and hydrocarbon fragments departure are certainly underestimated because of oxygen incorporation.

Aging also induces significant changes in UV-VisnIR spectra of EB. Typical EB spectrum consists of two absorption bands: the first at 320 nm ($\sim$ 3.8 eV) originates from the π–π^* transition in the benzenoïd rings, and the second at 640 nm ($\sim$ 1.9 eV) is associated with the intrachain excitonic transition from the highest occupied energy levels (HOMO) (centered on the benzenoïd rings) to the lowest unoccupied energy level (LUMO) (centered on the quinoïd rings).[30,31] This last transition is the most affected by aging. The maximum of the absorption due to excitonic transition (640 nm) presents an hypsochromic displacement with aging time, which is linked to a decrease in the conjugation length.[32,33] This hypsochromic shift is mainly observed for air-aged samples (shown in Fig. 9), but is also present, to a smaller degree, in vacuum-aged samples. In the latter case the decrease in conjugation is less pronounced because tertiary amines created upon the degradation may participate in the conjugation via lone pair of electrons of the tertiary nitrogen atom. Chain scission and incorporation of carbonyl

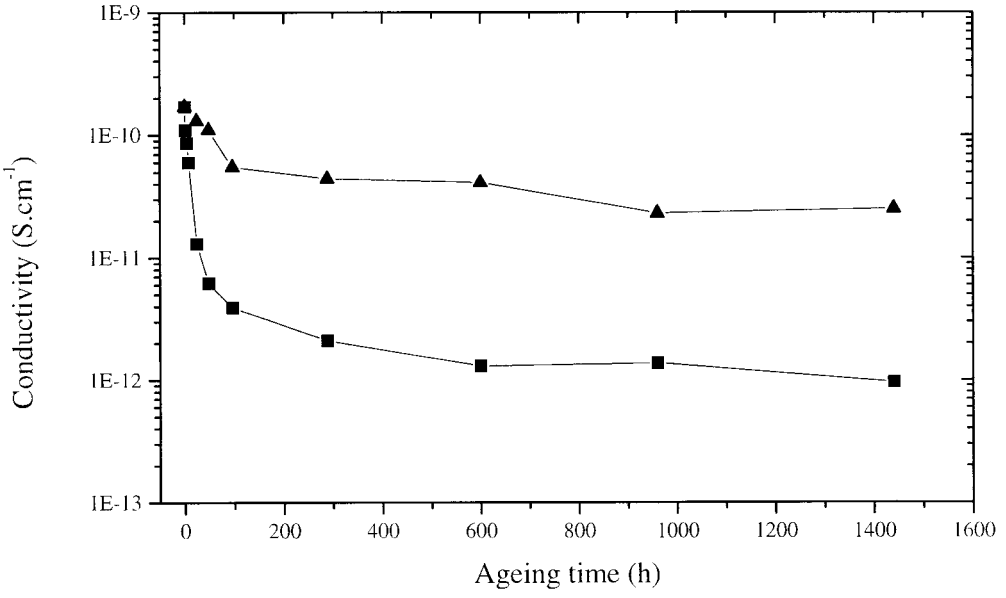

Figure 10 Conductivity for pressed pellets EB vs. aging time for (▲) powder aged under vacuum at 140°C and (■) powder aged in air at 140°C.

groups, additionally observed, during aging in air efficiently lower the conjugation length and act as charge carrier trapping centers. This is clearly manifested in the UV-Vis-nIR spectra.

The conductivity of pressed pellet aged EB has been monitored for both aging conditions, as shown in Figure 10. We observe a stronger loss of conductivity in the case of air aged samples compared to the vacuum-aged ones. Again, this decrease of conductivity can be correlated with the conjugation length decrease. This observation is rather obvious, because each conjugation breaking defect induces more charge localization and makes charge transport more difficult.

CONCLUSION

Complementary studies of EB degradation by elemental analysis, viscosity measurements, thermogravimetry, FTIR, XPS, and UV-Vis spectroscopies have shown that in the case of vacuum aging the dominant degradation mechanism consists of breaking of imine double bonds with simultaneous formation of tertiary amines and crosslinking. In air-aged samples in addition to the above-mentioned mechanism, other processes take place, namely oxygen incorporation in a form of ketone-type groups and chain scission. All these processes strongly influence the average conjugation length, and by consequence, the conductivity of the polymer, which decreases as a result of a decrease in charge carrier mobility.

The authors are grateful to Pr. Adam Pron for valuable discussions and critical reading of the manuscript. This work has been financially supported by the French government (MENRT).

References

1. Trivedi, D. C. Handbook of Organic Conductive Molecules and Polymers, Hari Singh Nalwa, Ed.; Wiley: New York, 1997, p. 2, and references therein.
2. Trivedi, D. C.; Dhawan, S. K. Polym. Adv. Technol 1993, 4, 335.
3. Wang, Y. Z.; Gebler, D. D.; Lin, L. B.; Blatchford, J. W.; Jessen, S. W.; Wang, H. L.; Epstein, A. J. Appl Phys Lett 1996, 68, 894.
4. Heeger, A. J.; Parker, I. D.; Yang, Y. Synth Met 1994, 67, 23.
5. (a) Cottevieille, D.; Le Mehaute, A.; Challioui, C.; Mirebeau, P.; Demay, J. N., Synth Met 1999, 101, 703. (b) Cottevieille, D.; Cariou, F.; Mirebeau, P.; Demay, J. N.; Parasie, Y. JICABLE99, 1999.
6. Djurado, D.; Gilles, B.; Rannou, P.; Travers, J. P. Synth Met 1999, 101, 803.
7. Rannou, P.; Nechtschein, M.; Travers, J. P.; Berner, D.; Wolter, A.; Djurado, D. Synth Met 1999, 101, 734.
8. Rannou, P.; Wolter, A.; Travers, J. P.; Gilles, B. Djurado, D. J. Chim Phys Phys Chim Biol 1998, 95, 1396.
9. Wolter, A.; Rannou, P.; Travers, J. P.; Gilles, B.; Djurado, D. Phys Rev B 1998, 58, 7637.
10. Jousseaume, V.; Morsli, M.; Bonnet, A. J Appl Phys 2000, 88, 960.
11. Pandey, S. S.; Gerard, M.; Sharma, A. L.; Malhotra, B. D. J Appl Polym Sci 2000, 75, 149.
12. Neoh, K. G.; Kang, E. T.; Tan, K. L. Thermochim Act 1990, 171, 292.
13. Lesueur, D.; Colin, X.; Alberola, N. D. Polym Bull 1997, 39, 755.
14. Matveeva, E. S. Synth Met 1996, 79, 127.
15. Pron, A.; Genoud, F.; Menardo, C.; Nechtschein, M. Synth Met 1988, 24, 193.
16. Holdcroft, S. J. Polym Sci B 1991, 29, 1585.
17. Allen, G.; Bevington, J. C. Comprehensive Polymer Science. The Synthesis, Characterization, Reactions and Applications of polymers; Booth, C.; Price, C., Eds.; Pergamon Press: Oxford, 1989.

18. Järvinen, H.; Laasko, J.; Auvinen, I.; Silvasti, E. Eur. Pat. Applic. No. 93120954.8 (1993).
19. Quillard, S.; Louarn, G.; Lefrant, S.; Macdiamid, A. G. Phys Rev B 1994, 50, 12496.
20. Chandrakanthi, N.; Careem, M. A. Polym Bull 2000, 44, 101.
21. Tanaka, S.; Iso, T. Polym Prepr 1997, 38, 207.
22. Lee, Y. M.; Kim, J. H.; Kang, J. S.; Ha, S. Y. Macromolecules 2000, 33, 7431.
23. Monkman, A. P.; Stevens, G. C.; Bloor, D. J Phys D Appl Phys 1991, 24, 738.
24. Liu, F. T.; Neoh, K. G.; Kang, E. T.; Han, H. S.; Tan, K. L. Polymer 1999, 40, 5285.
25. Demaret, X.; Cristallo, G.; Snauwaert, P.; Riga, J.; Verbist, J. J. Synth Met 1993, 55–57, 1051.
26. Kang, E. T.; Neoh, K. G.; Tan, K. L. Advances in Polymer Science; Springer-Verlag. Berlin, 1993, p. 136, vol. 106.
27. Scherr, E. M.; MacDiarmid, A. G.; Manohar, S. K.; Masters, J. G.; Sun, Y.; Tang, X.; Druy, M. A.; Glatkowski, P. J.; Calipe, V. B.; Fischer, J. E.; Cromack, K. R.; Jozefowicz, M. E.; Ginder, J. M.; McCall, R. P.; Epstein, A. J. Synth Met 1991, 41–43, 735.
28. Lopez, G. P.; Castner, D. G.; Ratner, B. D. Surface Interface Anal. 1991, 17, 267.
29. Handbook of X-Ray Photoelectron Spectroscopy, JEOL: Tokyo, Japan.
30. Duke, C. B.; Conwell, E. M.; Paton, A. Chem Phys Lett 1986, 131, 82.
31. Pomfret, S. J.; Rebourt, E.; Monkman, A. P. Synth Met 1996, 76, 19.
32. Neoh, K. G.; Kang, E. T.; Tan, K. L. Polymer 1992, 33, 2292.
33. Kuhn, H. J Chem Phys 1949, 17, 1198.